2023 62nd IEEE Conference on Decision and Control (CDC)
December 13-15, 2023. Marina Bay Sands, Singapore

Bearing-Based Formation Control Simultaneously Involving Several Heterogeneous Multi-Agent Systems with Nonlinear Uncertainties

Yujie Wang and Shuai Liu

***Abstract*— For a large-scale multi-agent system consisting of agents that have different types of dynamics, employing bearing rigidity theory to handle formation problems is unrealistic since the bearing-based rigid graph is extremely complicated and heterogeneous agents are hard to analyze as a whole. Therefore, we inventively propose to separate the large-scale system into smaller subsystems, and each subsystem is generated by agents which share the same dynamics. In such sense, formation control turns to focus on several systems with milder conditions rather than a system with complex analysis. The control objectives are to drive all systems to acquire the desired formation shapes, and make all systems simultaneously maneuver along with the desired velocities and maintain the formation shapes. To reduce communication cost, the leader-follower strategy is applied. To make formation control suitable for general environments, nonlinear uncertainties are considered, and the desired maneuvering velocities are time-varying. Adaptive nonsmooth distributed controllers are appropriately designed for all agents.**

I. INTRODUCTION

Formation control is of great importance in study of multi-agent systems, which focuses on cooperative behaviors that a group of agents collectively form specific geometrical shapes as a whole and maneuver along with common velocities together [1], [2]. At early stage, behavior-based [3], position-based [4] and virtual structure [5] methods are introduced into formation problems, but obvious mathematical limitations in these methods restrict formation control from a wider application both in theoretical expansion and practical usage. To overcome limitations, recently, the graph rigidity theory is widely considered in formation control.

The graph rigidity theory includes branches of distance [7]–[9], bearing [10]–[12], angle [13]–[15] and ratio-of-distance (RoD) [16] rigidity. Different branches adopt different inter-vertex information to construct rigid graphs in different senses, e.g., the bearing rigidity employs bearing information between neighboring agents to generate bearing-based rigid formation shapes. The bearing rigidity is evolved from the distance rigidity, then the angle and RoD rigidity are proposed enlightened by the bearing rigidity. Even though there have been bountiful studies of formation control based on different branches of graph rigidity theory (like [7]–[16]), they hardly focused on large-scale multi-agent systems combined by heterogeneous agents since the rigid graph is complicated and inter-agent information is hard to be unified if neighboring agents have different dynamics. Furthermore, situations that simultaneously involve several multi-agent systems are also really scarce. In this paper, these absent factors will be well considered by making connection between a large-scale system with heterogeneous agents and several systems, i.e., separating the large-scale into several heterogeneous subsystems. Comparing with other rigidity theory branches, the bearing rigidity is optimal, since: (i) distance-, angle- and RoD-based rigid graphs have rotational motion per se besides maneuvering, so that different systems may collide, (ii) angle- and RoD-based rigid graphs requires more complex constraints, and angle-based formation is only available in 2D and 3D spaces, and (iii) the distance rigidity only provides scalar information, while the bearing rigidity also provides vector information to determine relative directions between neighboring agents, which is helpful for orientation. These details are given in [8], [10], [14], [16].

Our contributions are: (i) inventively proposing to separate the large-scale system formed by heterogeneous agents into smaller homogeneous subsystems, (ii) analyzing formation control simultaneously involving several systems for the first time, (iii) considering nonlinear uncertainties and time-varying maneuvering targets to make formation control suitable for extensive situations, and (iv) building an extra velocity graph inspired by [14] to reduce computation cost.

Notations. All vectors are column vectors. $\|\cdot\|$ and $\|\cdot\|_1$ denote vector Euclidean norm and 1-norm, respectively. Let $\mathbf{1}_n = [1, \ldots, 1]^T \in \mathbb{R}^n$ and let $\mathbf{0}_n = [0, \ldots, 0]^T \in \mathbb{R}^n$. Let $I_n \in \mathbb{R}^{n\times n}$ be identity matrix. $\otimes$ denotes Kronecker product. For arbitrary matrix M used in d-dimensional space, denote $M^{\otimes} \triangleq M \otimes I_d$. Let $\mathrm{diag}(\cdot)$ be diagonal (or block diagonal) matrix. Let $|\mathcal{S}|$ be the cardinality of given set $\mathcal{S}$. Subscripts "[1]" and "[2]" in notations like $x_{[1]}$ and $x_{[2]}$ are employed to discern whether a notation involves single-integrator-based or double-integrator-based agent dynamics, respectively.

II. PRELIMINARIES

A. Graph and Framework

An undirected graph consisting of n vertices and m edges is denoted as $\mathcal{G} = (\mathcal{V}, \mathcal{E})$, where $\mathcal{V} = \{1, \ldots, n\}$ is vertex set and $\mathcal{E} \subset \mathcal{V} \times \mathcal{V}$ is edge set. The neighbor set of vertex i is $\mathcal{N}_i(\mathcal{E}) = \{j : (j, i) \in \mathcal{E}, j \in \mathcal{V}, j \neq i\}$. *Laplacian* matrix is $L = [l_{ij}]_{i,j=1}^n$, where $l_{ij} = 0$ if $j \notin \mathcal{N}_i(\mathcal{E})$, $l_{ij} = -1$ if $j \in \mathcal{N}_i(\mathcal{E})$, and $l_{ii} = \sum_{j\in\mathcal{N}_i(\mathcal{E})} 1$. The oriented graph is assigning orientation between neighboring agents in undirected graph which is still undirected graph, and let *incidence* matrix be $H = [h_{ki}]_{k=1,i=1}^{m,n}$, where $h_{ki} = 1$ if i is head vertex of edge k, $h_{ki} = -1$ if i is tail vertex of edge k, and $h_{ki} = 0$ otherwise. $\mathcal{G}$ is *connected* if and only

Yujie Wang and Shuai Liu are with the School of Control Science and Engineering, Shandong University, 250061 Ji'nan, Shandong, P.R. China. E-mails: yujie_wang@mail.sdu.edu.cn; liushuai@sdu.edu.cn.

if $\text{rank}(H) = n - 1$. Moreover, the *complete* graph of $\mathcal{G}$ is denoted as $\mathcal{G}_{\Im} = (\mathcal{V}, \mathcal{E}_{\Im})$ which ensures $\mathcal{N}_i(\mathcal{E}_{\Im}) = \mathcal{V}\backslash\{i\}$.

A framework in d-dimensional space is presented by $\mathcal{F} = (\mathcal{G}, p)$, where $p = [p_1^T, \ldots, p_n^T]^T \in \mathbb{R}^{nd}$ is the compact form generated by vertex's position $p_i \in \mathbb{R}^d$, $i = 1, \ldots, n$.

B. Bearing Rigidity Theory

Given a framework $\mathcal{F} = (\mathcal{G}, p)$, the bearing is defined as

$$g_{ij} \triangleq \frac{p_i - p_j}{\|p_i - p_j\|} = \frac{e_{ij}}{\|e_{ij}\|} \in \mathbb{R}^d, \tag{1}$$

where $e_{ij} \triangleq p_i - p_j$. Note that $g_{ij} = -g_{ji}$. Then, the bearing rigidity function $r_{\mathcal{G}}(p) : \mathbb{R}^{nd} \to \mathbb{R}^{md}$ is given by

$$r_{\mathcal{G}}(p) \triangleq [\ldots, g_{ji}^T, \ldots]^T \in \mathbb{R}^{md}, \quad (i, j) \in \mathcal{E}. \tag{2}$$

Based on (2), the bearing rigidity matrix $R(p)$ is determined by the Jacobian matrix of $r_{\mathcal{G}}(p)$ as

$$R(p) = \frac{\partial r_{\mathcal{G}}(p)}{\partial p} = \text{diag}\left(\frac{P(g_{ji})}{\|e_{ij}\|}\right) H^{\otimes} \in \mathbb{R}^{md \times nd}, \tag{3}$$

where $P(g_{ji}) \triangleq I_d - \frac{e_{ji}}{\|e_{ij}\|}\frac{e_{ji}^T}{\|e_{ij}\|}$ is an orthogonal projection. Then, we give a lemma that will be used in Section V.

Lemma 1. $R(p)\left(\mathbf{1}_n \otimes x\right) = \mathbf{0}_{md}$, $\forall x \in \mathbb{R}^d$.

Proof. Let $D_{\mathcal{G}}(p) = [\ldots, e_{ij}^T, \ldots]^T \in \mathbb{R}^{md}$, and then rewrite (3) as $R(p) = \frac{\partial r_{\mathcal{G}}(p)}{\partial D_{\mathcal{G}}(p)} \frac{\partial D_{\mathcal{G}}(p)}{\partial p}$. Since $\frac{\partial D_{\mathcal{G}}(p)}{\partial p}\left(\mathbf{1}_n \otimes x\right) = \mathbf{0}_{md}$ is proved in [6], $R(p)\left(\mathbf{1}_n \otimes x\right) = \frac{\partial r_{\mathcal{G}}(p)}{\partial D_{\mathcal{G}}(p)}\mathbf{0}_{md} = \mathbf{0}_{md}$. □

Bearing rigidity attributes is clarified through rank criteria of $R(p)$. Let $\mathcal{F}_{\Im} = (\mathcal{G}_{\Im}, p)$ be the *complete* framework of $\mathcal{F}$. $\mathcal{F}$ is defined to be *infinitesimally bearing rigid* if and only if $\text{rank}(R(p)) = nd - d - 1$. $\mathcal{F}$ is defined to be *bearing rigid* if and only if $\text{rank}(R(p)) = \text{rank}(R_{\Im}(p))$, where $R_{\Im}(p)$ is the bearing rigidity matrix of $\mathcal{F}_{\Im}$. $\mathcal{F}$ is defined to be *globally bearing rigid* if and only if $\mathcal{F}$ is *bearing rigid*. From [1], *global bearing rigidity* is important in formation control since it restricts $\mathcal{F}$ to be a unique geometrical shape.

Infinitesimal bearing rigidity has excellent properties that it: (i) implies *global bearing rigidity* that target geometrical formation shapes are able to be uniquely determined, and (ii) remains invariant even if the space dimension varies. Let the infinitesimal bearing motion of $\mathcal{F}(t) = (\mathcal{G}, p(t))$ be $p^{\iota} \triangleq \lim_{\Delta t \to 0} \frac{p(t+\Delta t) - p(t)}{\Delta t}$ that satisfies $R(p)p^{\iota} = \mathbf{0}_{md}$. The motion p^{ι} is *trivial* if p^{ι} are translational and/or scaling motions. An *infinitesimally bearing rigid* framework always maintains the bearing invariance under *trivial* motions, i.e., the shape of the framework remains unique in bearing-based sense which is described as $p(t_2) = cp(t_1) + \mathbf{1}_n \otimes \xi$, where $c \in \mathbb{R}\backslash\{0\}$, $\xi \in \mathbb{R}^d$, and t_1, t_2 are different points of time.

III. PROBLEM SKELETON

A. System Dynamics

The dynamics for single-integrator-based agents i are

$$\dot{p}_{[1]i} = u_{[1]i} + \Upsilon_i(p_{[1]i})\theta_i, \tag{4}$$

where $p_{[1]i} \in \mathbb{R}^d$ is position and $u_{[1]i} \in \mathbb{R}^d$ is control input. $\Upsilon_i(p_{[1]i}) \in \mathbb{R}^{d \times r}$ is a matrix consisting of continuous and bounded nonlinear functions with respect to $p_{[1]i}$, and $\theta_i \in \mathbb{R}^r$ is unknown parameter. For other double-integrator-based agents j, the dynamics are

$$\begin{aligned} \dot{p}_{[2]j} &= v_{[2]j} \\ \dot{v}_{[2]j} &= u_{[2]j} + \Phi_j(p_{[2]j}, v_{[2]j})\vartheta_j, \end{aligned} \tag{5}$$

where $p_{[2]j} \in \mathbb{R}^d$ is position, $v_{[2]j} \in \mathbb{R}^d$ is velocity and $u_{[2]j} \in \mathbb{R}^d$ is control input. $\Phi_j(p_{[2]j}, v_{[2]j}) \in \mathbb{R}^{d \times s}$ is a matrix consisting of continuous and bounded nonlinear functions with respect to $p_{[2]j}$ and $v_{[2]j}$, and $\vartheta_j \in \mathbb{R}^s$ is unknown parameter. In following sections, (4) and (5) will be in compact forms to depict whole multi-agent systems.

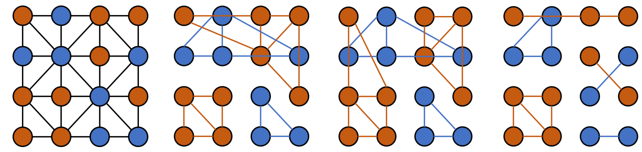

Fig. 1. Single-integrator-based agents (blue dots), and double-integrator-based agents (orange dots). (a) A hybrid multi-agent system with *infinitesimally bearing rigid* underlying topology. (b)-(d) examples of separation that all heterogeneous multi-agent systems still *infinitesimally bearing rigid*.

B. Multi-Agent System Separation

We consider *infinitesimally bearing rigid* graphs are used to construct underlying topologies for multi-agent systems which represent the communication conditions. To avoid misunderstanding, we define some significant conceptions.

Definition 1 (Homogeneous and Heterogeneous Agents)**.** Homogeneous agents mean that different agents have the same dynamics, while heterogeneous agents mean that different agents have different dynamics.

Definition 2 (Hybrid Multi-Agent System and Several Heterogeneous Multi-Agent Systems)**.** Hybrid multi-agent system means that single system is formed by heterogeneous agents. Several heterogeneous multi-agent systems mean that there are several systems together, and each system is formed only by homogeneous agents, but agents between different systems can be heterogeneous.

Fig. 1(a) shows a hybrid multi-agent system, and Fig. 1(b)-(d) gives examples of heterogeneous multi-agent systems. It is hard to use the bearing rigidity theory in large-scale hybrid multi-agent systems. Fig. 1(a) for example, there are two downsides: (i) it needs plethora of communication between agents since the *infinitesimally bearing rigid* graphs have too many edges, and (ii) hybrid systems are difficult to analyze in formation control. Thus, we separate the hybrid system and rebuild several smaller heterogeneous subsystems.

The separation process is: (i) classifying all the heterogeneous agents, (ii) restricting the scale of each subsystem, i.e., subdividing homogeneous agents into different subsystems, and (iii) ensuring each subsystem's underlying topology is *infinitesimally bearing rigid*. Fig. 1(b)-(d) give three examples of separation consequences.

This separation has advantages that: (i) the communication cost is largely decreased thanks to the stark decline of edges in underlying topologies, and (ii) bearing-based formation control is easy to fulfill when each system only contains few homogeneous agents. In this way, the bearing-based formation control simultaneously involves several heterogeneous multi-agent systems rather than a hybrid multi-agent system.

C. Problem Description

Given a hybrid multi-agent system in d-dimensional space with n heterogeneous agents, there are $n_{[1]}$ single-integrator-based agents and $n_{[2]}$ double-integrator-based agents, i.e., $n = n_{[1]} + n_{[2]}$. This hybrid system can be separated into k heterogeneous systems that contains $k_{[1]}$ single-integrator-based systems and $k_{[2]}$ double-integrator-based systems, i.e., $k = k_{[1]} + k_{[2]}$ $(k_{[1]}, k_{[2]} > 0)$. Let $\mathcal{G}_{[1]a} = (\mathcal{V}_{[1]a}, \mathcal{E}_{[1]a})$ be the underlying topology of the single-integrator-based system, where $a = 1, \ldots, k_{[1]}$ and $\sum_{a=1}^{k_{[1]}} |\mathcal{V}_{[1]a}| = n_{[1]}$. Similarly, let $\mathcal{G}_{[2]b} = (\mathcal{V}_{[2]b}, \mathcal{E}_{[2]b})$ be the underlying topology of the double-integrator-based system, where $b = 1, \ldots, k_{[2]}$ and $\sum_{b=1}^{k_{[2]}} |\mathcal{V}_{[2]b}| = n_{[2]}$. Besides, after separation, all the systems satisfy $2 \leq |\mathcal{V}_{[1]a}| \leq n_{[1]}$ and $2 \leq |\mathcal{V}_{[2]b}| \leq n_{[2]}$. The related frameworks are $\mathcal{F}_{[1]a} = (\mathcal{G}_{[1]a}, p_{[1]a})$ and $\mathcal{F}_{[2]b} = (\mathcal{G}_{[2]b}, p_{[2]b})$, where $p_{[1]a} = [\ldots, p_{[1]i}^T, \ldots]^T \in \mathbb{R}^{|\mathcal{V}_{[1]a}|}$, $i \in \mathcal{V}_{[1]a}$, and $p_{[2]b} = [\ldots, p_{[2]j}^T, \ldots]^T \in \mathbb{R}^{|\mathcal{V}_{[2]b}|}$, $j \in \mathcal{V}_{[2]b}$. These frameworks represent formtion shapes of multi-agent systems. Then, let $\mathcal{F}^*_{[1]a} = (\mathcal{G}_{[1]a}, p^*_{[1]a})$ and $\mathcal{F}^*_{[2]b} = (\mathcal{G}_{[2]b}, p^*_{[2]b})$ be the desired formation shapes where $p^*_{[1]a}$ and $p^*_{[2]b}$ are desired positions.

Assumption 1. Frameworks $\mathcal{F}^*_{[1]a}$ and $\mathcal{F}^*_{[2]b}$ are *infinitesimal bearing rigid*, where $a = 1, \ldots, k_{[1]}$ and $b = 1, \ldots, k_{[2]}$.

Remark 1. Unlike distance, angle, and RoD rigidity theories, in bearing rigidity theory, *collinear* cases are allowed in *infinitesimal bearing rigid* frameworks [10]. Therefore, the desired formation shapes are less restricted. *Collinear* cases are those that exist more than two neighboring agents collinear, and some *collinear* cases are given in Fig. 1(b)-(d).

We focus on the following formation control problem.

Problem 1. Given a hybrid multi-agent system, the formation control objectives are that after system separation and subsystem rebuilding, all heterogeneous subsystems: (i) will acquire the desired bearing-based formation shapes, and (ii) will simultaneously maneuver along with a desired velocity and maintain the desired formation shapes.

To deal with Problem 1, it should: (i) use Assumption 1 to generate the desired formation shapes for all subsystems, and (ii) use the leader-follower strategy and additionally create a velocity-sensing graph to lessen communication cost.

IV. PROBLEM ANALYSIS

A. System Dynamics Analysis

System dynamics are considered in term of compact forms corresponding to (4) and (5). To design formation controllers, relative measurement is embedded. By compact form notations, the bearing errors are

$$\begin{aligned} \delta_{[1]a} &= g_{[1]a} - g^*_{[1]a} \in \mathbb{R}^{|\mathcal{E}_{[1]a}|d}, \quad a = 1, \ldots, k_{[1]}, \\ \delta_{[2]b} &= g_{[2]b} - g^*_{[2]b} \in \mathbb{R}^{|\mathcal{E}_{[2]b}|d}, \quad b = 1, \ldots, k_{[2]}, \end{aligned} \tag{6}$$

and the unknown parameter estimations are

$$\begin{aligned} \tilde{\theta}_a &= \theta_a - \hat{\theta}_a \in \mathbb{R}^{|\mathcal{V}_{[1]a}|r}, \quad a = 1, \ldots, k_{[1]}, \\ \tilde{\vartheta}_b &= \vartheta_b - \hat{\vartheta}_b \in \mathbb{R}^{|\mathcal{V}_{[1]b}|s}, \quad b = 1, \ldots, k_{[2]}, \end{aligned} \tag{7}$$

where $\hat{\theta}_a$ and $\hat{\vartheta}_b$ are estimates of θ_a and ϑ_b, respectively. Moreover, since the velocity state $v_{[2]}$ from (5) cannot be directly accessed in double-integrator-based dynamics, the velocity-level fictitious control is introduced as

$$z_{[2]b} = v_{[2]b} - \check{v}_{[2]b} \in \mathbb{R}^{|\mathcal{V}_{[2]b}|d}, \ b = 1, \ldots, k_{[2]}, \tag{8}$$

where $\check{v}_{[2]b}$ is fictitious control law and $z_{[2]b}$ is velocity error.

B. Leader-Follower Strategy with Velocity Graph

The leader-follower strategy can lessen communication cost to satisfy velocity consensus [17]. Let vertex $\{0\}$ be the transmitter that generates the desired velocity $v^*(t) \in \mathbb{R}^d$.

Assumption 2. The time-varying $v^*(t)$ satisfies: (i) $v^*(t) \in \mathcal{L}_\infty$, and (ii) $v^*(t)$ is of class C^1 with $\sup_{t\geq 0}\|\dot{v}^*(t)\| \leq \sigma$, where σ is positive constant.

While [11] sets two leader agents which are initialized at desired positions and spontaneously generate desired velocities, we loosen such strict conditions. For each system, there is only one leader agent which is randomly initialized and directly accesses the transmitter $\{0\}$ to learn the desired velocity. Leader sets are $\overline{\mathcal{V}}_{[1]a} = \{1\}$, $a = 1, \ldots, k_{[1]}$ and $\overline{\mathcal{V}}_{[2]b} = \{1\}$, $b = 1, \ldots, k_{[2]}$. Follower sets are $\underline{\mathcal{V}}_{[1]a} = \{2, \ldots, |\mathcal{V}_{[1]a}|\}$, $a = 1, \ldots, k_{[1]}$ and $\underline{\mathcal{V}}_{[2]b} = \{2, \ldots, |\mathcal{V}_{[2]b}|\}$, $b = 1, \ldots, k_{[2]}$. Fig. 2(a) explains how to assign the leader-follower strategy for all the heterogeneous systems.

Actually, velocity consensus can be held in an easier way rather than use bearing-based underlying topologies. We set an extra topology namely velocity graph as $\mathcal{G}^v = (\mathcal{V}^v, \mathcal{E}^v)$ to communicate velocity information between neighboring agents. $\mathcal{G}^v$ contains several subgraphs $\mathcal{G}^v_{[1]a} = (\mathcal{V}_{[1]a}, \mathcal{E}^v_{[1]a})$ and $\mathcal{G}^v_{[2]b} = (\mathcal{V}_{[2]b}, \mathcal{E}^v_{[2]b})$ which illustrate the inner velocity graphs for all the heterogeneous systems. Thus, $\mathcal{V}^v = \{0\} \cup \left(\bigcup_{a=1}^{k_{[1]}} \mathcal{V}_{[1]a}\right) \cup \left(\bigcup_{b=1}^{k_{[2]}} \mathcal{V}_{[2]b}\right)$, and $\mathcal{E}^v = \mathcal{E}^{\overline{\mathcal{V}}}_0 \cup \left(\bigcup_{a=1}^{k_{[1]}} \mathcal{E}^v_{[1]a}\right) \cup \left(\bigcup_{b=1}^{k_{[2]}} \mathcal{E}^v_{[2]b}\right)$ with $\mathcal{E}^{\overline{\mathcal{V}}}_0 = \{(i, 0) : i \in \mathcal{N}_0(\mathcal{E}^v)\}$.

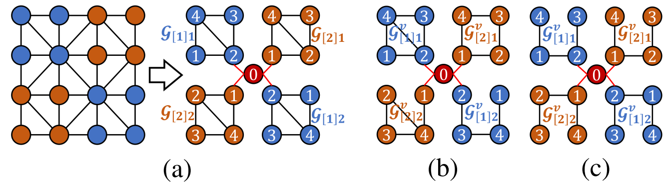

Fig. 2. Single-integrator-based agents (blue dots), double-integrator-based agents (orange dots), and leader agents connecting with transmitter $\{0\}$ by red edges. (a) Assignment of leader-follower strategy after system separation and rebuilding. (b)-(c) Two available cases of $\mathcal{G}^v$ under Assumption 3.

Assumption 3. The velocity graph $\mathcal{G}^v$: (i) is undirected and *connected*, (ii) includes a spanning tree with the root vertex $\{0\}$, and (iii) $\mathcal{E}^v_{[1]a} \subset \mathcal{E}_{[1]a}$, $a = 1, \ldots, k_{[1]}$, and $\mathcal{E}^v_{[2]b} \subset \mathcal{E}_{[2]b}$, $b = 1, \ldots, k_{[2]}$.

Remark 2. For each system, the desired formation shape can be unique only when underlying topology is *infinitesimally bearing rigid*. However, the velocity consensus can be ensured in many cases when each agent can learn the desired velocity by communicating with others, i.e., $\mathcal{G}^v$ is available when *connected*. Fig. 2(b)-(c) show available cases of $\mathcal{G}^v$. The velocity consensus analysis is under $\mathcal{G}^v$, but (8) is excepted as state $v_{[2]b}$ is an inner state of system dynamics.

Based on $\mathcal{G}^v$, the maneuvering velocity errors are

$$\begin{aligned} \tilde{v}_{[1]a} &= \hat{v}_{[1]a} - \mathbf{1}_{|\mathcal{V}_{[1]a}|} \otimes v^*, \quad a = 1, \ldots, k_{[1]}, \\ \tilde{v}_{[2]b} &= \hat{v}_{[2]b} - \mathbf{1}_{|\mathcal{V}_{[2]b}|} \otimes v^*, \quad b = 1, \ldots, k_{[2]}, \end{aligned} \tag{9}$$

where $\hat{v}_{[1]a} \in \mathbb{R}^{|\mathcal{V}_{[1]a}|d}$ and $\hat{v}_{[2]b} \in \mathbb{R}^{|\mathcal{V}_{[2]b}|d}$ are velocity estimates, $\tilde{v}_{[1]a}$ and $\tilde{v}_{[2]b}$ are maneuvering velocity errors. To mathematically distinguish leader and follower agents, we denote $D_{[1]a} = \operatorname{diag}(\ldots, d_{[1]i}, \ldots)$, $i \in \mathcal{V}_{[1]a}$ and $D_{[2]b} = \operatorname{diag}(\ldots, d_{[2]j}, \ldots)$, $j \in \mathcal{V}_{[2]b}$, where $d_{[1]i} = 1$ (resp. $d_{[2]j}$=1) if $i \in \overline{\mathcal{V}}_{[1]a}$ (resp. $j \in \overline{\mathcal{V}}_{[2]b}$), and $d_{[1]i} = 0$ (resp. $d_{[2]j}$=0) if $i \in \underline{\mathcal{V}}_{[1]a}$ (resp. $j \in \underline{\mathcal{V}}_{[2]b}$), then give the following definition.

Definition 3. The *leader-follower coalescent* matrix is defined as $C_{[1]a} = L^v_{[1]a} + D_{[1]a}$ (resp. $C_{[2]b} = L^v_{[2]b} + D_{[2]b}$) with $a = 1, \ldots, k_{[1]}$ (resp. $b = 1, \ldots, k_{[2]}$), where $L^v_{[1]a}$ and $L^v_{[2]b}$ are *Laplacian* matrices of $\mathcal{G}^v_{[1]a}$ and $\mathcal{G}^v_{[2]b}$, respectively. Note that $C_{[1]a}$ and $C_{[2]b}$ are positive definite since $D_{[1]a}$, $D_{[2]b}$ and *Laplacian* matrices are semi-positive definite.

V. FORMATION CONTROLLER DESIGN

In $\mathbb{R}^d$ space, the formation controllers for all agents in different systems ensure: (i) $\delta_{[1]a} \to \mathbf{0}_{|\mathcal{E}_{[1]a}|d}$ and $\delta_{[2]b} \to \mathbf{0}_{|\mathcal{E}_{[2]b}|d}$ as $t \to \infty$, and (ii) $\tilde{v}_{[1]a} \to \mathbf{0}_{|\mathcal{V}_{[1]a}|d}$ and $\tilde{v}_{[2]b} \to \mathbf{0}_{|\mathcal{V}_{[2]b}|d}$ as $t \to \infty$, where $a = 1, \ldots, k_{[1]}$ and $b = 1, \ldots, k_{[2]}$.

A. Single-Integrator-Based Controller

As all the single-integrator-based multi-agent systems have the similar dynamics, we choose one system to analyze, and the controllers in this system also fit in other systems.

For a certain system $\mathcal{F}_{[1]a} = (\mathcal{G}_{[1]a}, p_{[1]a})$ with the inner velocity graph $\mathcal{G}^v_{[1]a} = (\mathcal{V}_{[1]a}, \mathcal{E}^v_{[1]a})$ where $a \in \{1, \ldots, k_{[1]}\}$, we select a Lyapunov function as

$$V_{[1]a} = \underbrace{\frac{1}{2}\left(\delta^T_{[1]a}\delta_{[1]a} + \tilde{\theta}^T_a \varGamma^{-1}_a \tilde{\theta}_a\right)}_{V_1} + \underbrace{\frac{1}{2}\tilde{v}^T_{[1]a} C^{\otimes}_{[1]a}\tilde{v}_{[1]a}}_{V_2}, \tag{10}$$

where $\varGamma_a = \operatorname{diag}(\varGamma_1, \ldots, \varGamma_{|\mathcal{V}_{[1]a}|}) \in \mathbb{R}^{|\mathcal{V}_{[1]a}|r \times |\mathcal{V}_{[1]a}|r}$ is positive definite, and $C_{[1]a}$ is in Definition 3. Involving the compact form of (4), the time derivative of (10) is

$$\begin{aligned} \dot{V}_{[1]a} =& \delta^T_{[1]a}\dot{\delta}_{[1]a} - \tilde{\theta}^T_a \varGamma^{-1}_a \dot{\hat{\theta}}_a + \tilde{v}^T_{[1]a} C^{\otimes}_{[1]a}\dot{\tilde{v}}_{[1]a} \\ =& \delta^T_{[1]a} R_{[1]a}\left(u_{[1]a} + \varUpsilon_a \theta_a\right) - \tilde{\theta}^T_a \varGamma^{-1}_a \dot{\hat{\theta}}_a \\ &+ \tilde{v}^T_{[1]a} C^{\otimes}_{[1]a}\left(\dot{\hat{v}}_{[1]a} - \mathbf{1}_{|\mathcal{V}_{[1]a}|} \otimes \dot{v}^*\right), \end{aligned} \tag{11}$$

where $\varUpsilon_a = \operatorname{diag}(\ldots, \varUpsilon_i(p_{[1]i}), \ldots)$, $i \in \mathcal{V}_{[1]a}$, $R_{[1]a} \triangleq R(p_{[1]a})$ is used to simplify the notation, and the fact $\dot{\delta}_{[1]a} = R_{[1]a}\dot{p}_{[1]a}$ is involved based on (3). Then, we design

$$\begin{aligned} u_{[1]a} &= -\gamma_1 R^T_{[1]a}\delta_{[1]a} - \varUpsilon_a \hat{\theta}_a + \hat{v}_{[1]a} \\ \dot{\hat{\theta}}_a &= \varGamma_a \varUpsilon^T_a R^T_{[1]a}\delta_{[1]a}, \end{aligned} \tag{12}$$

where $\gamma_1 > 0$ is control gain. By employing (12) and Lemma 1, (11) becomes

$$\begin{aligned} \dot{V}_{[1]a} =& \underbrace{-\gamma_1 \delta^T_{[1]a} R_{[1]a} R^T_{[1]a}\delta_{[1]a} + \delta^T_{[1]a} R_{[1]a}\tilde{v}_{[1]a}}_{\dot{V}_1} \\ &\underbrace{+ \tilde{v}^T_{[1]a} C^{\otimes}_{[1]a}\left(\dot{\hat{v}}_{[1]a} - \mathbf{1}_{|\mathcal{V}_{[1]a}|} \otimes \dot{v}^*\right)}_{\dot{V}_2}. \end{aligned} \tag{13}$$

Next, based on (13), we design

$$\dot{\hat{v}}_{[1]a} = -(C^{\otimes}_{[1]a})^{-1} R^T_{[1]a}\delta_{[1]a} - \gamma_2 \operatorname{sgn}\big(C^{\otimes}_{[1]a}\tilde{v}_{[1]a}\big), \tag{14}$$

where $\gamma_2 > 0$ is control gain, and $\operatorname{sgn}(\cdot)$ is signum vector that all entries are signum functions. Equation (14) makes $\dot{\tilde{v}}_{[1]a} = \dot{\hat{v}}_{[1]a} - \mathbf{1}_{|\mathcal{V}_{[1]a}|} \otimes \dot{v}^* \triangleq f(\tilde{v}_{[1]a}, t) \in K[f](\tilde{v}_{[1]a}, t)$, where $K[f](\cdot)$ is a compact, convex, nonempty, upper semi-continuous set-valued map defined in [18]. Employing (14) and differential inclusion [18] into (13) renders

$$\dot{V}_{[1]a} = \dot{V}_1 + \dot{V}_2 \overset{a.e.}{\in} \dot{V}_1 + \dot{\tilde{V}}_2, \tag{15}$$

where $a.e.$ means "almost everywhere", and $\dot{\tilde{V}}_2$ is given by

$$\begin{aligned} \dot{\tilde{V}}_2 =& \bigcap\nolimits_{\varpi \in (\partial V_2 / \partial \tilde{v}_{[1]a})} \varpi^T K[f](\tilde{v}_{[1]a}, t) \\ \subset& -\tilde{v}^T_{[1]a} R^T_{[1]a}\delta_{[1]a} - \tilde{v}^T_{[1]a} C^{\otimes}_{[1]a}\left(\mathbf{1}_{|\mathcal{V}_{[1]a}|} \otimes \dot{v}^*\right) \\ &- \gamma_2 \tilde{v}^T_{[1]a} C^{\otimes}_{[1]a} K\left[\operatorname{sgn}\big(C^{\otimes}_{[1]a}\tilde{v}_{[1]a}\big)\right] \\ =& -\tilde{v}^T_{[1]a} R^T_{[1]a}\delta_{[1]a} - \tilde{v}^T_{[1]a} C^{\otimes}_{[1]a}\left(\mathbf{1}_{|\mathcal{V}_{[1]a}|} \otimes \dot{v}^*\right) \\ &- \gamma_2 \tilde{v}^T_{[1]a} C^{\otimes}_{[1]a} \operatorname{sgn}^{\dagger}\big(C^{\otimes}_{[1]a}\tilde{v}_{[1]a}\big) \\ =& -\tilde{v}^T_{[1]a} R^T_{[1]a}\delta_{[1]a} - \gamma_2 \|C^{\otimes}_{[1]a}\tilde{v}_{[1]a}\|_1 \\ &+ (\dot{v}^*)^T \sum\nolimits_{i=1}^{|\mathcal{V}_{[1]a}|d}\left(C^{\otimes}_{[1]a}\tilde{v}_{[1]a}\right)_i \\ \le& -\tilde{v}^T_{[1]a} R^T_{[1]a}\delta_{[1]a} - \gamma_2 \|C^{\otimes}_{[1]a}\tilde{v}_{[1]a}\|_1 \\ &+ \|\dot{v}^*\|_1 \cdot \|C^{\otimes}_{[1]a}\tilde{v}_{[1]a}\|_1 \\ \le& -\tilde{v}^T_{[1]a} R^T_{[1]a}\delta_{[1]a} - (\gamma_2 - \sigma)\|C^{\otimes}_{[1]a}\tilde{v}_{[1]a}\|_1, \end{aligned} \tag{16}$$

in which σ is in Assumption 2, and each entry of $\operatorname{sgn}^{\dagger}(\cdot)$ is defined as $\operatorname{sgn}^{\dagger}(x_i)$ with $\operatorname{sgn}^{\dagger}(x_i) = 1$ if $x_i > 0$, $\operatorname{sgn}^{\dagger}(x_i) = -1$ if $x_i < 0$, and $\operatorname{sgn}^{\dagger}(x_i) = [-1, 1]$ if $x_i = 0$. Therefore,

$$\begin{aligned} \dot{V}_{[1]a} &\le -\gamma_1 \delta^T_{[1]a} R_{[1]a} R^T_{[1]a}\delta_{[1]a} - (\gamma_2 - \sigma)\|C^{\otimes}_{[1]a}\tilde{v}_{[1]a}\|_1 \\ &\le -\gamma_1 \lambda\big(R_{[1]a}R^T_{[1]a}\big)\|\delta_{[1]a}\|^2 - (\gamma_2 - \sigma)\|C^{\otimes}_{[1]a}\tilde{v}_{[1]a}\|_1, \end{aligned} \tag{17}$$

where $\lambda(\cdot) > 0$ is the minimum eigenvalue since $R_{[1]a}$ has full row rank which implies $R_{[1]a}R^T_{[1]a}$ is positive definite.

According to (17), $\dot{V}_{[1]a} < 0$ if $\sigma < \gamma_2$, so that controllers combined with (12) and (14) are valid when $\sigma < \gamma_2$. Besides, [10] has verified that the bearing rigidity matrix $R_{[1]a}$ (which is defined by (3) as $R(p) = \mathrm{diag}\big(P(g_{ji})/\|e_{ij}\|\big)H^{\otimes})$ can be replaced by a simplified matrix $\bar{R}_{[1]a}$ (which is given by the form like $\bar{R}(p) = \mathrm{diag}\big(P(g_{ji})\big)H^{\otimes}$). Substituting $\bar{R}_{[1]a}$ into controllers helps reduce computation cost as relative position measurement $\|e_{ij}\|$ is omitted. Under the condition $\sigma < \gamma_2$, the controllers for the whole systems become

$$\begin{aligned} u_{[1]a} &= -\gamma_1 \bar{R}^T_{[1]a}\delta_{[1]a} - \Upsilon\hat{\theta}_a + \hat{v}_{[1]a} \\ \dot{\hat{v}}_{[1]a} &= -(C^{\otimes}_{[1]a})^{-1}\bar{R}^T_{[1]a}\delta_{[1]a} - \gamma_2 \mathrm{sgn}\big(C^{\otimes}_{[1]a}\tilde{v}_{[1]a}\big) \\ \dot{\hat{\theta}}_a &= \Gamma_a \Upsilon^T_a \bar{R}^T_{[1]a}\delta_{[1]a}, \end{aligned} \tag{18}$$

and agent-wise controllers can be extracted from (18) as

$$\begin{aligned} u_{[1]i} =& -\gamma_1\zeta_{[1]i} - \Upsilon_i\hat{\theta}_i + \hat{v}_{[1]i} \\ \dot{\hat{v}}_{[1]i} =& -(C^{\otimes}_{[1]a})^{-1}_i \zeta_{[1]i} \\ & - \gamma_2 \mathrm{sgn}\Big(d_i(\hat{v}_{[1]i} - v^*) + \sum_{j\in\mathcal{N}_i(\mathcal{E}^v_{[1]a})}\big(\hat{v}_{[1]i} - \hat{v}_{[1]j}\big)\Big) \\ \dot{\hat{\theta}}_i =& \Gamma_i \Upsilon^T_i \zeta_{[1]i}, \end{aligned} \tag{19}$$

where $i \in \mathcal{V}_{[1]a}$, $\zeta_{[1]i} \triangleq \sum_{j\in\mathcal{N}_i(\mathcal{E}_{[1]a})} P(g_{ij})g^*_{ij}$, $(C^{\otimes}_{[1]a})^{-1}_i \in \mathbb{R}^{d\times|\mathcal{V}_{[1]a}|d}$ is a submatrix given by the $(di-d+1)$-th to the di-th rows of $(C^{\otimes}_{[1]a})^{-1}$, $a = 1,\ldots,k_{[1]}$, and $\sigma < \gamma_2$ is held.

B. Double-Integrator-Based Controller

Since the controller design is similar to Section V-A, this part is simplified. For a certain system $\mathcal{F}_{[2]b} = (\mathcal{G}_{[2]b}, p_{[2]b})$ with the inner velocity graph $\mathcal{G}^v_{[2]b} = (\mathcal{V}_{[2]b}, \mathcal{E}^v_{[2]b})$ where $b \in \{1,\ldots,k_{[2]}\}$, we select a Lyapunov function as

$$V_{[2]b} = \frac{1}{2}\Big(\delta^T_{[2]b}\delta_{[2]b} + z^T_{[2]b}z_{[2]b} + \tilde{\vartheta}^T_b\Gamma^{-1}_b\tilde{\vartheta}_b + \tilde{v}^T_{[2]b}C^{\otimes}_{[2]b}\tilde{v}_{[2]b}\Big), \tag{20}$$

where $\Gamma_b = \mathrm{diag}(\Gamma_1,\ldots,\Gamma_{|\mathcal{V}_{[2]b}|}) \in \mathbb{R}^{|\mathcal{V}_{[2]b}|s\times|\mathcal{V}_{[2]b}|}$ is positive definite, and $C_{[2]b}$ is in Definition 3. Involving the compact form of (5), the time derivative of (20) is

$$\begin{aligned} \dot{V}_{[2]b} =& \delta^T_{[2]b}R_{[2]b}\left(z_{[2]b} + \check{v}_{[2]b}\right) + z^T_{[2]b}\left(u_{[2]b} + \Phi_b\vartheta_b\right) \\ & + \tilde{v}^T_{[2]b}C^{\otimes}_{[2]b}\Big(\dot{\hat{v}}_{[2]b} - \mathbf{1}_{|\mathcal{V}_{[2]b}|}\otimes\dot{v}^*\Big) - \tilde{\vartheta}^T_b\Gamma^{-1}_b\dot{\hat{\vartheta}}_b, \end{aligned} \tag{21}$$

where $\Phi_b = \mathrm{diag}(\ldots,\Phi_i(p_{[2]i}),\ldots)$, $i \in \mathcal{V}_{[2]b}$, $R_{[2]b} \triangleq R(p_{[2]b})$, and $\dot{\delta}_{[2]b} = R_{[2]b}\dot{p}_{[2]b} = R_{[2]b}v_{[2]b}$. Then, we design

$$\begin{aligned} u_{[2]b} &= -\gamma_3 z_{[2]b} - R^T_{[2]b}\delta_{[2]b} - \Phi_b\hat{\vartheta}_b \\ \check{v}_{[2]b} &= -\gamma_4 R^T_{[2]b}\delta_{[2]b} + \hat{v}_{[2]b} \\ \dot{\hat{v}}_{[2]b} &= -(C^{\otimes}_{[1]a})^{-1}R^T_{[2]b}\delta_{[2]b} - \gamma_5\mathrm{sgn}\big(C^{\otimes}_{[2]b}\tilde{v}_{[2]b}\big) \\ \dot{\hat{\vartheta}}_b &= \Gamma_b\Phi^T_b z_{[2]b}, \end{aligned} \tag{22}$$

where $\gamma_3, \gamma_4, \gamma_5 > 0$ are control gains. Then, (21) becomes

$$\begin{aligned} \dot{V}_{[2]b} \le& -\gamma_3\|z_{[2]b}\|^2 - \gamma_4\lambda\big(R_{[2]b}R^T_{[2]b}\big)\|\delta_{[2]b}\|^2 \\ & - (\gamma_5 - \sigma)\,\|C^{\otimes}_{[2]b}\tilde{v}_{[2]b}\|_1, \end{aligned} \tag{23}$$

where $\lambda(\cdot) > 0$ is the minimum eigenvalue. Similar to (18), the bearing rigidity matrix $R_{[2]b}$ in (22) can be also replaced by $\bar{R}_{[2]b}$ which omits relative position measurement $\|e_{ij}\|$ to reduce computational cost. After replacement, when $\sigma < \gamma_5$, the agent-wise controllers are

$$\begin{aligned} u_{[2]i} =& -\gamma_3 z_{[2]i} - \zeta_{[2]i} - \Phi_i\hat{\vartheta}_i \\ \check{v}_{[2]i} =& -\gamma_4\zeta_{[2]i} + \hat{v}_{[2]i} \\ \dot{\hat{v}}_{[2]i} =& -(C^{\otimes}_{[2]b})^{-1}_i\zeta_{[2]i} \\ & - \gamma_5\mathrm{sgn}\Big(d_i(\hat{v}_{[2]i} - v^*) + \sum_{j\in\mathcal{N}_i(\mathcal{E}^v_{[2]b})}(\hat{v}_{[2]i} - \hat{v}_{[2]j})\Big) \\ \dot{\hat{\vartheta}}_i =& \Gamma_i\Phi^T_i z_{[2]i}, \end{aligned} \tag{24}$$

where $i \in \mathcal{V}_{[2]b}$, $\zeta_{[2]i} \triangleq \sum_{j\in\mathcal{N}_i(\mathcal{E}_{[2]b})} P(g_{ij})g^*_{ij}$, $(C^{\otimes}_{[2]b})^{-1}_i \in \mathbb{R}^{d\times|\mathcal{V}_{[2]b}|d}$ is a submatrix given by the $(di-d+1)$-th to the di-th rows of $(C^{\otimes}_{[2]b})^{-1}$, $b = 1,\ldots,k_{[2]}$, and $\sigma < \gamma_5$ is held.

VI. SIMULATION

By using adaptive distributed controllers (19) and (24) for agents in heterogeneous systems, **Problem 1** can be solved in $\mathbb{R}^d$ space. We consider a simulation example in 2D plane, while the desired formation shape is given by Fig. 2(a) and the velocity graph is given by Fig. 2(c). Initial positions for all agents are random (we also consider *collinear* cases here). Let desired velocity be $v^*(t) = [1, -0.5\mathrm{cos}t]^T$. The single-integrator-based agent dynamics are given by

$$\dot{p}_{[1]i} = u_{[1]i} + \sin(p_{[1]i})\theta_i, \quad i \in \mathcal{V}_{[1]a}, a = 1, 2,$$

where $\theta_i \in \mathbb{R}$ is unknown parameter. The double-integrator-based agent dynamics with nonlinear uncertainties are

$$\begin{aligned} \dot{p}_{[2]j} &= v_{[2]j} \\ \dot{v}_{[2]j} &= u_{[2]j} + [\sin(p_{[2]j}), \sin(v_{[2]j})]\vartheta_j, \quad j \in \mathcal{V}_{[2]b}, b = 1, 2, \end{aligned}$$

where $\vartheta_j \in \mathbb{R}^2$ is unknown parameter.

Fig. 3 verifies that distributed controllers (19) and (24) can drive all heterogeneous systems to acquire desired formation shapes and make all the systems simultaneously maneuver along with the desired velocity while maintaining the formation shapes. It is worth noting that unique formation shapes in bearing-based sense can have different scales as mentioned in Section II-B, which means the control objectives are fulfilled as shown in Fig. 3 despite existing different scales. Fig. 4 shows convergence performances which verify all the closed-loop heterogeneous systems are asymptotically stable.

VII. CONCLUSIONS AND FUTURE WORKS

The bearing rigidity theory is employed into formation control. Since a large-scale hybrid multi-agent system including agents that have different types of dynamics is difficult to handle, the innovation of system separation and rebuilding is introduced to make the formation control simultaneously involve several heterogeneous multi-agent systems, which lessens communication cost and improves the formation feasibility of complex hybrid systems. Adaptive nonsmooth distributed controllers are appropriately designed both for single-integrator-based and double-integrator-based agents to fulfill the formation control objectives when nonlinear uncertainties exist and the desired velocities are time-varying.

The future work will study how to make all the systems have the same formation shapes without different scales.

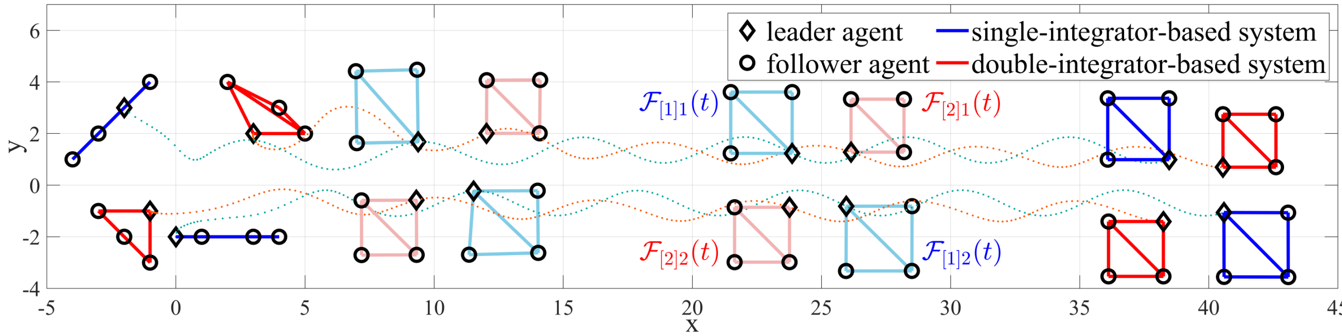

Fig. 3. Bearing-based formation trajectories simultaneously involving 4 heterogeneous multi-agent systems with desired $v^*(t) = [1, -0.5\text{cos}t]^T$, where control gains $\gamma_1, \gamma_3, \gamma_4 = 1 > 0$, $\gamma_2 = 3$ and $\gamma_5 = 4.5$ with $\gamma_2, \gamma_5 > \sigma \geq \sup_{t \geq 0} \|\dot{v}^*(t)\|$.

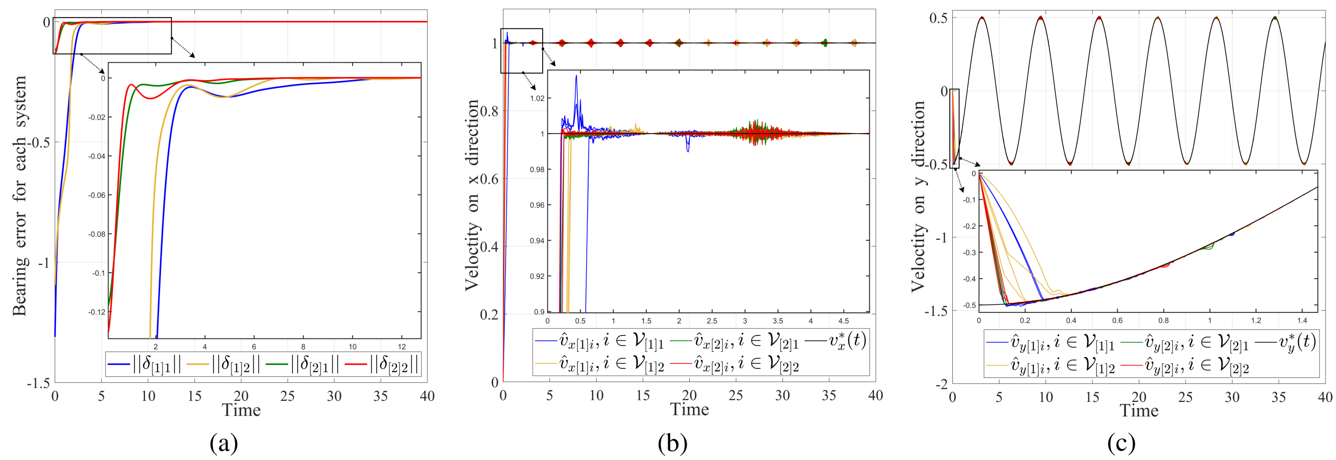

Fig. 4. (a) Total bearing error for each system in form of Euclidean norm. (b) Velocity tracking performance for each agent on x direction with desired $v_x^*(t) = 1$. (c) Velocity tracking performance for each agent on y direction with desired $v_y^*(t) = -0.5\text{cos}t$.

References

[1] K. K. Oh, M. C. Park and H.S. Ahn, "A survey of multi-agent formation control," *Automatica*, vol. 53, pp. 424-440, 2015.

[2] X. Wang, X. Li and Z. Zheng, "Survey of developments on multi-agent formation control related problems," *Journal of Control and Decision*, vol. 28, no. 11, pp. 1601-1613, 2013.

[3] J. R. T. Lawton, R. W. Beard and B. J. Young, "A decentralized approach to formation maneuvers", *IEEE Transactions on Robotics and Automation*, vol. 19, no. 6, pp. 3210-3230, 2003.

[4] S. Coogan and M. Arcak, "Scaling the size of a formation using relative position feedback", *Automatica*, vol. 48, no. 10, pp. 2677-2685, 2012.

[5] W. Ren and R. W. Beard, "Formation feedback control for multiple spacecraft via virtual structures", *IEE Proceedings - Control Theory and Applications*, vol. 151, no. 3, pp. 357-368, 2004.

[6] M. Queiroz, X. Y. Cai and M. Feemster. *Formation control of multi-agent systems : A graph rigidity approach*. John Wiley & Sons, 2019.

[7] B. D. O. Anderson, C. Yu, B. Fidan and J. M. Hendrickx, "Rigid graph control architectures for autonomous formations," *IEEE Control Systems Magazine*, vol. 28, no. 6, pp. 48-63, 2008.

[8] K. K. Oh and H. S. Ahn, "Formation control of mobile agents based on inter-agent distance dynamics," *Automatica*, vol. 47, no. 10, pp. 2306-2312, 2011.

[9] Z. Y. Sun, M. C. Park, B. D. O. Anderson and H. S. Ahn, "Distributed stabilization control of rigid formations with prescribed orientation," *Automatica*, vol. 78, pp. 250-257, 2017.

[10] S. Zhao and D. Zelazo, "Bearing rigidity and almost global bearing-Only formation stabilization," *IEEE Transactions on Automatic Control*, vol. 61, no. 5, pp. 1255-1268, 2016.

[11] S. Zhao and D. Zelazo, "Translational and scaling formation maneuver control via a bearing-based approach," *IEEE Transactions on Control of Network Systems*, vol. 4, no. 3, pp. 429-438, 2017.

[12] X. Li, C. Wen and C. Chen, "Adaptive formation control of networked robotic systems with bearing-only measurements," *IEEE Transactions on Cybernetics*, vol. 51, no. 1, pp. 199-209, 2021.

[13] G. Jing, G. Zhang, H. W. Lee and L. Wang, "Angle-based shape determination theory of planar graphs with application to formation stabilization," *Automatica*, vol. 105, pp. 117-129, 2019.

[14] L. Chen and M. Cao, "Angle Rigidity for Multi-Agent Formations in 3D," *IEEE Transactions on Automatic Control*, doi: 10.1109/TAC.2023.3237799, 2023.

[15] L. M. Chen, L. H. Xie, X. L. Li, X. Fang and M. Feroskhan, "Simultaneous localization and formation using angle-only measurements in 2D," *Automatica*, vol. 146, 2022.

[16] K. Cao, Z. Han, X. Li and L. Xie, "Ratio-of-distance rigidity theory with application to similar formation control," *IEEE Transactions on Automatic Control*, vol. 65, no. 6, pp. 2598-2611, 2020.

[17] H. Zhi, L. Chen, C. Li and Y. Guo, "Leader-follower affine formation control of second-order nonlinear uncertain multi-agent systems," *IEEE Transactions on Circuits and Systems II-Express Briefs*, vol. 68, no. 12, pp. 3547-3551, 2021.

[18] D. Shevitz and B. Paden, "Lyapunov stability theory of nonsmooth systems," *IEEE Transactions on Automatic Control*, vol. 39, no. 9, pp. 1910-1914, 1994.